

Reduction of the residual compressive stress of tetrahedral amorphous carbon film by Ar background gas during the filtered vacuum arc process

Tae-Young Kim,^{a)} Churl Seung Lee,^{b)} Young Jin Lee,^{c)} and Kwang-Ryeol Lee^{d)}
Future Technology Research Division, Korea Institute of Science and Technology, P.O. Box 131, Cheongryang, Seoul 136-791, Korea

Keun-Hwa Chae
Division of Materials Science, Korea Institute of Science and Technology, P.O. Box 131, Cheongryang, Seoul 136-791, Korea

Kyu Hwan Oh
School of Materials Science and Engineering, Seoul National University, Shinrim-dong, Seoul 151-742, Korea

(Received 7 August 2006; accepted 23 September 2006; published online 17 January 2007)

Tetrahedral amorphous carbon (ta-C) film was prepared by the filtered vacuum arc process with Ar background gas. The residual compressive stress of the film decreased significantly as the Ar flow rate increased, whereas negligible change in the mechanical properties was observed. Structure analysis by Raman spectroscopy, near edge x-ray absorption fine structure, and electron spin resonance spectra revealed a close relationship between the residual compressive stress and the bond distortion that invokes paramagnetic defects or unpaired π electrons. These results demonstrate that the stress reduction can occur by relaxation of the distorted or twisted atomic bonds at the same fraction of sp^3 hybridized bonds, which enhances the stability of the ta-C coating without deterioration in the advantageous properties. The effect of Ar background gas is discussed in terms of the increased ion population of low kinetic energy in the plasma beam. © 2007 American Institute of Physics. [DOI: 10.1063/1.2408385]

I. INTRODUCTION

The high residual compressive stress of tetrahedral amorphous carbon (ta-C) film deposited by the filtered vacuum arc (FVA) process causes instability of the coating and substantially limits its applications. The high residual stress is a matter of particular concern for its application to microelectromechanical systems (MEMS) because the MEMS structure can be severely deformed even when very thin ta-C film is deposited. Systematic control of the residual stress has thus been one of the most important issues in ta-C coating technology. However, a decrease in the residual compressive stress is usually accompanied by the deterioration of the advantageous properties such as high hardness, optical transparency, or surface smoothness. This behavior can be understood by considering that most advantages of the ta-C film originate from the high fraction of sp^3 hybridized bonds, which induces significant bond distortion in the amorphous

structure.¹⁻³ Therefore, it has been a challenging issue to reduce the residual compressive stress while keeping the useful properties of the ta-C film.

There have been only a few reports of residual stress being successfully reduced without significant structural degradation. As an example, Friedman *et al.* reported the stress free ta-C film prepared by postthermal annealing of highly stressed film.⁴ They observed by electron energy loss spectroscopy (EELS) analysis that the stress reduction occurred without significant change in the fraction of sp^3 hybridized bonds. Even though the mechanism for independent control of the residual stress is not fully addressed, this result suggests that another structural factor should be considered in addition to the sp^3 bond fraction. Similar results were reported with boron incorporated films or a multilayer of differently structured films.^{2,5,6} In the present work, we investigated the residual stress and atomic bond structure of the ta-C film deposited by a FVA process with Ar background gas. We observed that the residual stress decreased significantly as the Ar gas was introduced into the reaction chamber. On the other hand, only minor changes in the fraction of sp^3 bonds and the mechanical properties were observed. Structure analysis by near edge x-ray absorption fine structure (NEXAFS) and electron spin resonance (ESR) spectra showed that the Ar background gas results in the relaxation of distorted or twisted atomic bonds without significant change in the fraction of sp^3 hybridized bonds.

^{a)}Also at School of Materials Science and Engineering, Seoul National University, Shinrim-Dong, Seoul 151-742, Korea.

^{b)}Present address: Nano technology based Information and Energy Storage Research Center, Korea Electronics Technology Institute, 68 Yatap-dong, Bundang-gu, Seongnam-si, Gyeonggi-do 463-816, Korea.

^{c)}Present address: Development Purchasing Unit DSC Development Center, Samsung Techwin, JungWon-gu, Seongnam-si, Gyeonggi-do 462-121, Korea.

^{d)}Author to whom correspondence should be addressed; FAX: +82-2-958-5494; electronic mail: krlee@kist.re.kr

II. EXPERIMENT

ta-C film was deposited using a FVA of solid graphite. The arc plasma was generated at the graphite target of dc potential of 50 V with respect to the electrically ground anode or reactor wall. The plasma was guided to the reaction chamber after magnetic filtering of macroparticles. Details of the vacuum arc source are given elsewhere.³ A Si (100) wafer of 510 μm thickness was used for the substrate. The Si wafer was placed on an electrically ground water-cooled substrate holder. A thin Si (100) strip of $100 \pm 5 \mu\text{m}$ thickness was also used as the substrate to measure the residual stress of the film. During deposition, Ar was introduced using a mass flow controller at a flow rate ranging from 0.5 to 6 SCCM (standard cubic centimeters per minute). The base pressure of the reaction chamber was 6×10^{-4} Pa. When the vacuum arc was generated without Ar flow, the chamber pressure increased to 1.5×10^{-3} Pa. The deposition pressure rapidly increased to 6.0×10^{-2} Pa as the Ar flow rate increased to 2 SCCM, followed by a slow increase to 1.0×10^{-1} Pa at an Ar flow rate of 6 SCCM. The deposition rate of films decreased from 1.0 to 0.7 nm/min as the Ar background gas increased from 0 to 6 SCCM. The film thickness was fixed at 120 nm in all specimens by adjusting the deposition time.

The residual stress in the film was calculated from the curvature of the film/substrate composite using Stoney's equation.⁷ The thickness of the deposited film was measured by an α -step profilometer employing a step made by a shadow mask. A nanoindenter (Nano Indenter II of Nano Instruments, Inc.) in the continuous stiffness measurement (CSM) mode was used to measure the hardness and the elastic modulus of the film. Because very thin ta-C film was deposited on the Si substrate, it is hard to completely exclude the substrate effect in the nanoindentation measurement. However, if the effect of the residual stress is correctly considered, the measured values can be qualitatively compared because films of the same thickness were deposited on the same substrate. The composition of the deposited film was analyzed by Rutherford backscattering spectrometry (RBS) using a 2 MeV collimated $^4\text{He}^{2+}$ ion beam. The atomic bond structure was characterized using NEXAFS. NEXAFS spectra were obtained in a soft x-ray beam line (7B1) at the Pohang Accelerator Laboratory. The paramagnetic defect density of the sample was measured at room temperature with an x-band (9.9 GHz) ESR spectrometer. An MgOMn²⁺ standard sample with a known total number of defects, 1.1×10^{15} , was adopted as the reference for quantitative analysis of the defects.

III. RESULTS AND DISCUSSION

The RBS spectra of the film showed that all the films are composed solely of carbon. No Ar peak was observed in the RBS spectra of the films deposited with Ar background gas. Because of the high sensitivity of RBS to heavy elements in a light matrix, it can be said that almost no Ar was incorporated in the film regardless of the Ar gas flow rate. (Upper limit of the Ar concentration would be less than 0.1 at. % as confirmed by the spectrum simulations.) On the other hand,

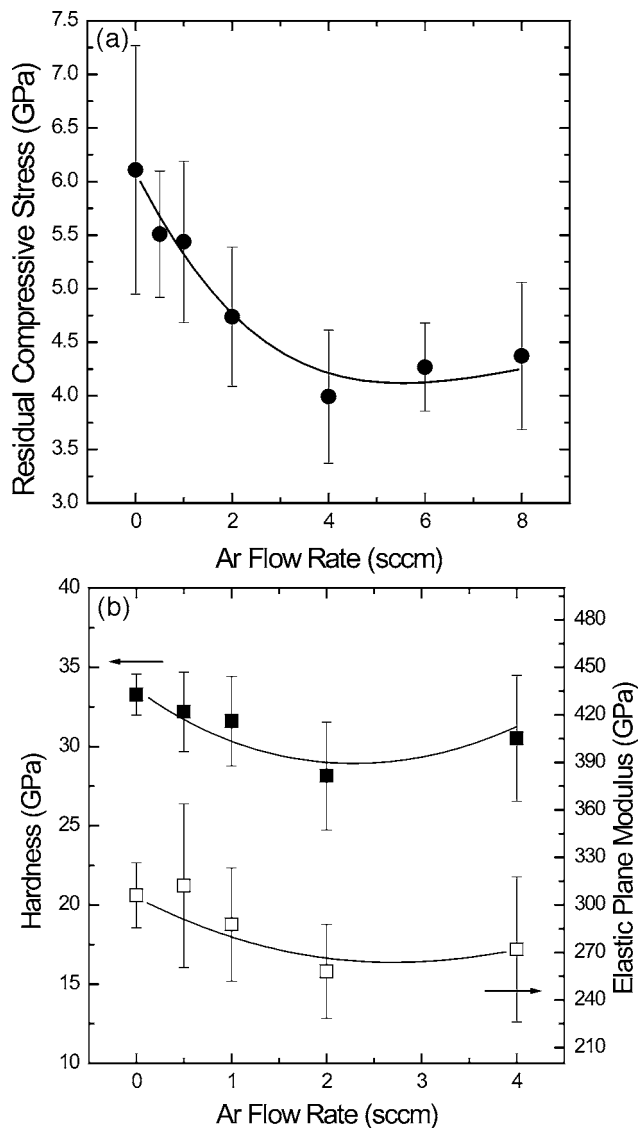


FIG. 1. Dependence of the mechanical properties on the Ar flow rate in the deposition condition: (a) residual compressive stress and (b) hardness and elastic plane modulus.

the residual compressive stress in the film decreased significantly as the Ar flow rate increased, as shown in Fig. 1(a). Errors in the residual stress data of Fig. 1(a) are mainly due to the uncertainty in the thickness of the film. In spite of the errors, it is evident that the residual compressive stress appreciably decreased by 35% (from 6.3 to 4.2 GPa) as the Ar flow rate increased from 0 to 4 SCCM. With further increases in the Ar flow rate, the residual compressive stress was saturated at about 4.2 GPa. Figure 1(b) shows the hardness and the plane strain modulus of the film for various Ar flow rates. In contrast to the residual compressive stress, the changes in the mechanical properties occurred within a much smaller range. As the Ar flow rate increased from 0 to 4 SCCM, the hardness decreased from 33 to 30.5 GPa and the plane strain modulus from 306 to 271 GPa. Considering the effect of the residual stress on the nanoindentation measurement,⁸ one would further suggest that the change in the mechanical properties is much smaller than indicated by the measured range, 10%.

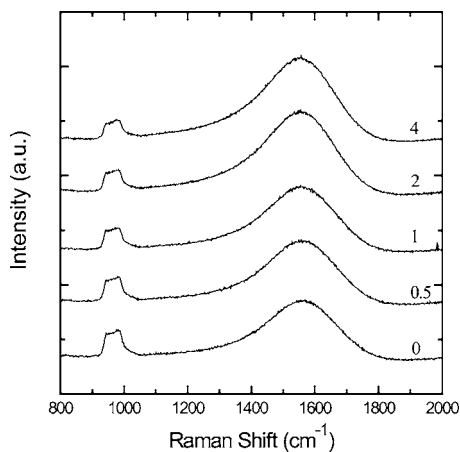


FIG. 2. Raman spectra of ta-C films for various values of the Ar flow rate.

It is well known that the hardness of the amorphous carbon film is proportional to the degree of three-dimensional interlinks of the sp^2 clusters in the carbon network.⁹ The residual stress can also increase with the interlinks, because the distortion of atomic bond angles and/or lengths should be proportional to the degree of the interlinks in covalently bonded amorphous materials. If the reduction in the residual stress is attributed to the decreasing number of three-dimensional interlinks, the mechanical properties would also be degraded. It is evident in Fig. 1 that the Ar gas flow during the FVA process provides a way of reducing the residual compressive stress of ta-C film without significant change in the three-dimensional interlinks.

Figure 2 shows the Raman spectra of the ta-C film for various Ar flow rates. The numbers on the spectra are the Ar flow rate in SCCM. The spectra are shifted upward for ease of comparison. The shapes of the spectra are essentially the same for all Ar flow rates and are typical of ta-C film: an almost symmetric carbon Raman peak near 1550 cm^{-1} with the secondary peak of the Si substrate at about 950 cm^{-1} due to the optical transparency of the film.^{10,11} The G -peak position of the carbon Raman peak was in the range of $1543 \pm 5\text{ cm}^{-1}$ regardless of the Ar flow rate. (During the Raman spectrum analysis, we considered the effect of the residual stress on the G -peak position as reported by Shin *et al.*¹⁰) It is empirically known that the G -peak position shifts to a higher wave number as the fraction of sp^3 hybridized bonds decreases.⁶ Hence, the Raman spectrum analysis shows that the fraction of sp^3 hybridized bonds in the film is independent of the Ar flow rate.

The atomic bond structure of the film or the fraction of sp^2 and sp^3 hybridized bonds can be characterized in detail by NEXAFS spectroscopy, because the π^* resonance is well separated in energy from the rest of the resonance in the carbon K edge spectra.^{12,13} Figure 3(a) shows the NEXAFS spectra for various Ar flow conditions. All spectra were normalized to the maximum peak at about 296 eV and shifted upward for ease of comparison. Numbers on the spectra are the Ar flow rates in SCCM. For comparison, the graphite spectrum is also included. All the spectra have a peak at 284 eV corresponding to the transition from $C\ 1s \rightarrow \pi^*$ state of sp and sp^2 sites.¹² (The π^* peak shifts downward by 1 eV

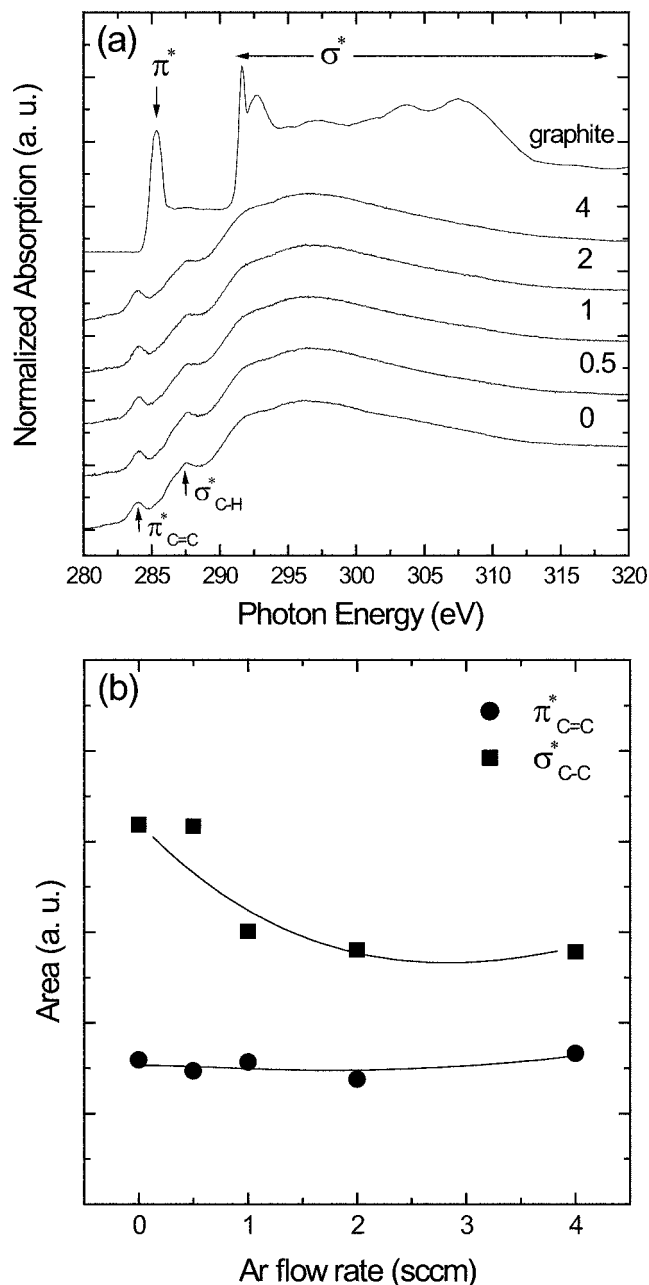


FIG. 3. (a) NEXAFS spectra of the ta-C films for various values of the Ar flow rate. (b) Dependence of π^* and σ_{C-H}^* peak intensity on the Ar flow rate.

from 285 eV for graphite. The shift is presumably due to the residual stress in the film, as can be deduced from an annealing experiment with ta-C film.¹⁴) In most ta-C films, the content of $C \equiv C$ bonds corresponding to sp hybridization is so small that the peak at 284 eV can be considered to be due only to $C=C$ double bonds or sp^2 sites.^{15,16} Hence, the peak intensity can be used to judge the content of sp^2 hybridized bonds in the film. Because of the higher content of sp^3 bonds in the ta-C films, the intensity of the $\pi_{C=C}^*$ peaks of the film is much smaller than that in graphite. The peak at 287 eV corresponds to the σ_{C-H}^* transition of the $C-H$ bonds that would originate from absorption of hydrocarbon to the surface dangling bonds after exposure to ambient air.¹⁷ The broad band between 290 and 310 eV results from an overlapping $C\ 1s \rightarrow \sigma^*$ transition at sp^2 and/or sp^3 sites. The

amorphous structure of the ta-C film would cause broadening of the σ resonance. These characteristic peaks are consistent with those observed in previous work.¹⁴

Figure 3(b) is the peak intensity of the $\pi^*_{C=C}$ and σ^*_{C-H} resonances for various Ar flow rates. The intensities were obtained by integrating the peak after correcting for the background. The intensity of the $\pi^*_{C=C}$ peaks is independent of the Ar flow rate, which shows that the sp^2/sp^3 fraction in the film or the degree of three-dimensional interlink is not extensively changed by the Ar flow. This is consistent with the Raman spectrum analysis and the minor changes in the mechanical properties shown in Fig. 1(b). In contrast, the intensity of the σ^*_{C-H} peak monotonically decreases with increasing Ar flow rate. Lee *et al.* showed that the σ^*_{C-H} peak is closely related to the defects in the film, which enhance the number of surface dangling bonds.¹⁴ The present NEXAFS analysis thus suggests that the Ar background gas reduced the defects in the ta-C film without significant change in the atomic bond structure.

A decrease in defects was also confirmed by the decrease in the ESR signal originating from paramagnetic defects. Figure 4(a) shows the ESR spectra for various Ar flow rates. The peaks at 3435 and 3520 G are those of the MgOMn²⁺ reference sample. The g factors of the spectra were 2.0028 ± 0.0003 , similar to the values for other forms of carbon.¹⁸ It is evident that the defects in the film monotonically decreased with increasing Ar flow rate. For quantitative analysis, the total number of defects in the film was calculated by comparing the peak intensity with that of the reference MgOMn²⁺ sample. The defect density, defined by the number of defects divided by the volume of the carbon film, is summarized in Fig. 4(b). The defect density in the film deposited without Ar flow was $4.95 \times 10^{21}/\text{cm}^3$. The defect density rapidly decreased to $3.2 \times 10^{21}/\text{cm}^3$ as the Ar flow increased to 1 SCCM, and was saturated on further increasing the Ar flow rate.

Structural analysis shows that the density of paramagnetic defects in ta-C film decreased with increasing Ar flow rate, whereas the ratio of sp^2/sp^3 or the degree of three-dimensional interlinks remained constant. This structural change would occur when the distorted bonds are relaxed during the deposition, because the misorientation between π orbitals corresponding to a bent or twisted bond creates paramagnetic defects.^{19,20} For example, relaxation of the highly distorted sp^2 clusters results in a decreasing number of unpaired π electrons and thus a smaller ESR signal. Relaxation of the twisted sp^2 bonds would also reduce the ESR signal. It must be noted that these relaxation processes can occur without a significant change in the three-dimensional interlinks. Hence, the present experimental observation of the residual stress and mechanical properties can be said to arise from the relaxation of the distorted bonds at the same degree of three-dimensional interlinks.

The present experiments using Ar background gas provided deposition conditions where bond distortion and the corresponding unpaired π electrons are reduced without a significant change in the three-dimensional interlinks. In order to understand the Ar background gas effect on the film structure, we characterized the ion beam by using a home-

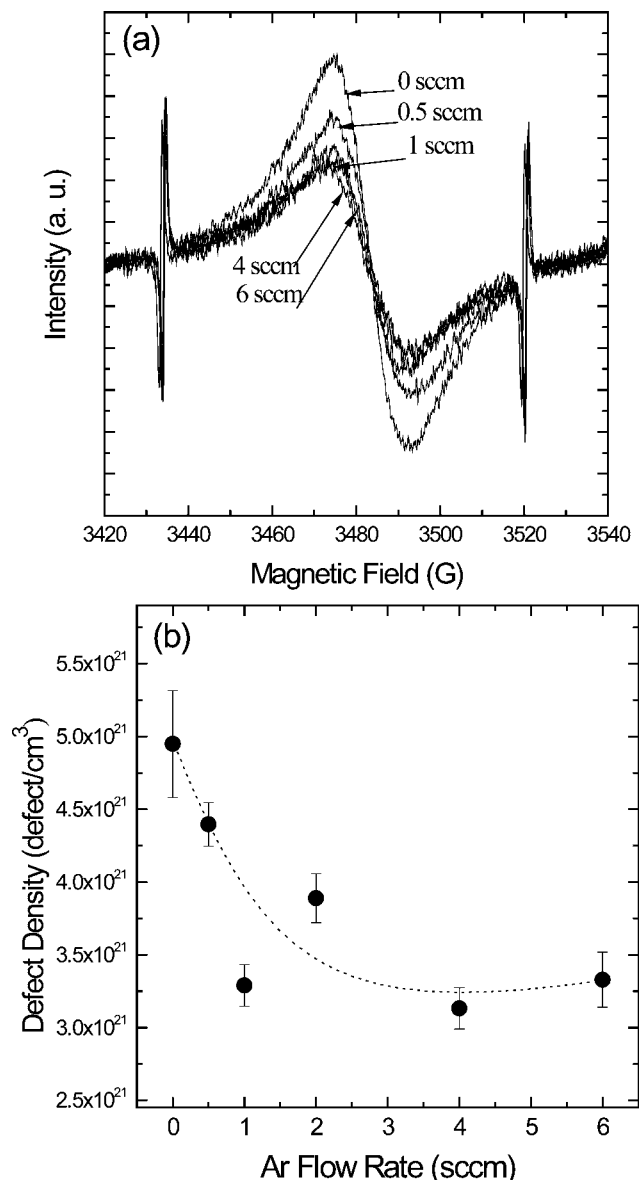


FIG. 4. (a) ESR spectra at the various Ar gas flow rates introduced into the chamber during deposition. (b) Dependence of the paramagnetic defect density on the Ar flow rate.

made Faraday cup where a retarding grid was installed 3.5 mm from the surface of an ion collector plate of diameter 10 mm. Figure 5 shows the dependence of the beam current density on the retarding grid potential (V_r) for various Ar flow rates. The measured beam current was corrected by considering contributions of the secondary electrons generated by the bombarding C and Ar ions. As the Ar flow rate increased, the total beam current measured at $V_r=0$ V increased. However, increasing the retarding potential led to a decreasing current as the Ar flow rate increased, which means that the population of the low kinetic energy ions becomes larger with increasing Ar gas flow. Considering that the film growth rate decreased with the Ar flow rate, one would suggest that the Ar background gas increased the number of ions of low kinetic energy that bombard the growing surface but does not participate in the film growth.

A possible reason for the present structural change with Ar gas flow would be a “massage” effect of the low kinetic

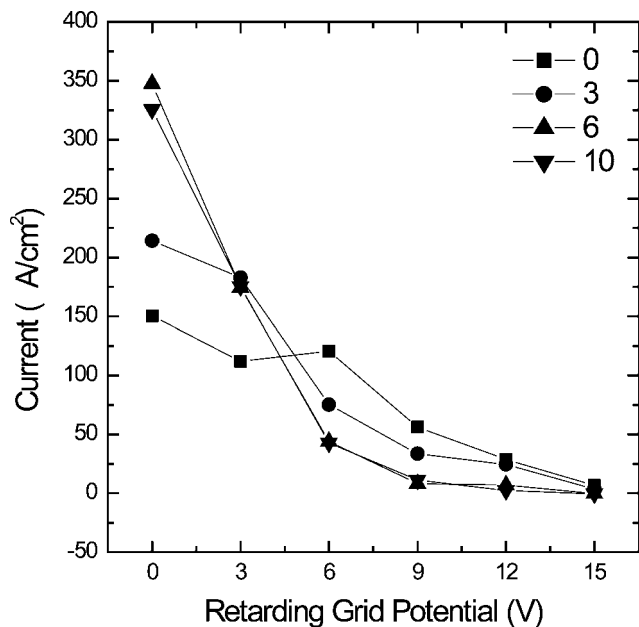


FIG. 5. Dependence of the beam current density on the retarding grid potential (V_r) for various Ar flow rates.

energy ions. Ar atoms in the background would decrease the mean free path of the carbon ion, which affects both the kinetic energy and its dispersion of the deposited ions. In addition, Ar atoms can also be ionized because of the abundance of electrons in the vacuum arc environment. These effects would generate low energy ions of both C and Ar, which bombard the deposited surface to supply the kinetic energy required to relax the distorted bond. If the energy of the ions is not sufficient to break the C–C bonds, the ion bombardment will not significantly change the atomic bond characteristics such as the sp^3/sp^2 ratio.

IV. CONCLUSIONS

Ar background gas during the FVA process provided a deposition condition where the distorted bonds are relaxed while three-dimensional interlinks in the amorphous carbon network are maintained. Under this experimental condition, the residual stress decreased without significant deterioration in the hardness or the elastic modulus. The present results

reveal a close relationship between the residual stress and the distorted bonds that invoke paramagnetic defects or unpaired π electrons. Relaxation of the distorted bonds makes it possible to increase the stability of the ta-C coating without sacrificing the useful physical properties.

ACKNOWLEDGMENTS

This research was supported by a grant (Code No. 06K1501-01610) from “Center for Nanostructured Materials Technology” under “21st Century Frontier R&D Programs” of the Ministry of Science and Technology, Korea, and Taewoong-Medical Co. Ltd.

¹Y. Lifshitz, G. D. Lempert, and E. Grossman, *Phys. Rev. Lett.* **72**, 2753 (1994).

²M. Chhowalla, Y. Yin, G. A. J. Amaratunga, D. R. McKenzie, and T. Frauenheim, *Appl. Phys. Lett.* **69**, 2344 (1996).

³C. S. Lee, K.-R. Lee, K. Y. Eun, K. H. Yoon, and J. H. Han, *Diamond Relat. Mater.* **11**, 198 (2002).

⁴T. A. Friedmann, J. P. Sullivan, J. A. Knapp, D. R. Tallant, D. M. Follstaedt, D. L. Medlin, and P. B. Mirkarimi, *Appl. Phys. Lett.* **71**, 3820 (1997).

⁵C. S. Lee, K.-R. Lee, and S.-H. Suh, *Mater. Sci. Technol.* **20**, 993 (2004).

⁶M. A. Tamor and W. C. Vassell, *J. Appl. Phys.* **76**, 3823 (1994).

⁷S. A. Brenner and S. Senderoff, *J. Res. Natl. Bur. Stand.* **42**, 105 (1949).

⁸Y. H. Lee, D. Kwon, and J. I. Jang, *Int. J. Mod. Phys. B* **17**, 1141 (2003).

⁹K.-R. Lee, M.-G. Kim, S.-J. Cho, K. Y. Eun, and T.-Y. Seong, *Thin Solid Films* **308–309**, 263 (1997).

¹⁰J.-K. Shin, C. S. Lee, K.-R. Lee, and K. Y. Eun, *Appl. Phys. Lett.* **78**, 631 (2001).

¹¹C. S. Lee, T.-Y. Kim, K.-R. Lee, J.-P. Ahn, and K. H. Yoon, *Chem. Phys. Lett.* **380**, 774 (2003).

¹²C. Lenardi, P. Piseri, V. Briois, C. E. Bottani, A. L. Bassi, and P. Milani, *J. Appl. Phys.* **85**, 7159 (1999).

¹³J. Kikuma, K. Yoneyama, M. Nomura, T. Konishia, T. Hashimoto, R. Mitsumoto, Y. Ohuchi, and K. Seki, *J. Electron Spectrosc. Relat. Phenom.* **88–91**, 919 (1998).

¹⁴C. S. Lee, J. K. Shin, K. Y. Eun, K.-R. Lee, and K. H. Yoon, *J. Appl. Phys.* **95**, 4829 (2004).

¹⁵C. Lenardi, M. A. Baker, V. Briois, L. Nobili, P. Piseri, and W. Gissler, *Diamond Relat. Mater.* **8**, 595 (1999).

¹⁶G. Comelli, J. Stöhr, C. J. Robinson, and W. Jark, *Phys. Rev. B* **38**, 7511 (1988).

¹⁷J. Diaz, S. Anders, X. Zhou, E. J. Moler, S. A. Kellar, and Z. Hussain, *J. Electron Spectrosc. Relat. Phenom.* **101–103**, 545 (1999).

¹⁸E. G. Gerstner, P. B. Lukins, D. R. McKenzie, and D. G. McCulloch, *Phys. Rev. B* **54**, 14504 (1996).

¹⁹U. Stephan, T. Frauenheim, P. Blaudeck, and G. Jungnickel, *Phys. Rev. B* **50**, 1489 (1994).

²⁰J. Robertson, *Mater. Sci. Eng., R.* **37**, 129 (2002).